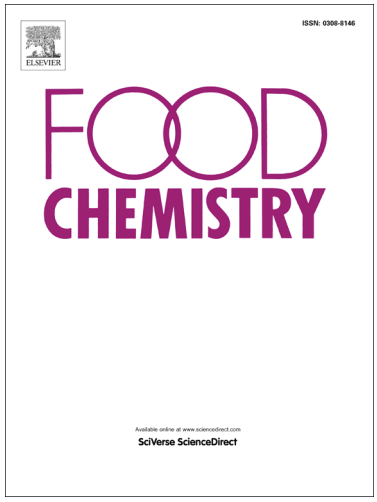

Formulation and characterization of astaxanthin-enriched nanoemulsions stabilized using ginseng saponins as natural emulsifiers

Gaofeng Shu, Nauman Khalid, Zhang Chen, Marcos A. Neves, Colin J. Barrow, Mitsutoshi Nakajima

PII: S0308-8146(18)30298-X
DOI: https://doi.org/10.1016/j.foodchem.2018.02.062
Reference: FOCH 22446

To appear in: *Food Chemistry*

Received Date: 24 October 2017
Revised Date: 27 January 2018
Accepted Date: 12 February 2018

Please cite this article as: Shu, G., Khalid, N., Chen, Z., Neves, M.A., Barrow, C.J., Nakajima, M., Formulation and characterization of astaxanthin-enriched nanoemulsions stabilized using ginseng saponins as natural emulsifiers, *Food Chemistry* (2018), doi: https://doi.org/10.1016/j.foodchem.2018.02.062

Formulation and characterization of astaxanthin-enriched nanoemulsions stabilized using ginseng saponins as natural emulsifiers

Gaofeng Shu[a□], Nauman Khalid[b,c,d*□], Zhang Chen[a], Marcos A. Neves [a,c], Colin J. Barrow[b], Mitsutoshi Nakajima[a,c]

[a]Tsukuba Life Science Innovation Program (T-LSI), University of Tsukuba, 1-1-1 Tennodai, Tsukuba, Ibaraki 305-8572, Japan

[b]Centre for Chemistry and Biotechnology, Deakin University, Waurn Ponds, Victoria 3217, Australia

[c]Graduate School of Life and Environmental Sciences, University of Tsukuba, 1-1-1 Tennodai, Tsukuba, Ibaraki 305-8572, Japan

[d]School of Food and Agricultural Sciences, University of Management and Technology, Lahore 54000, Pakistan

□These authors work equally in conducting experiments

---

* To whom correspondence should be addressed.

E-mail: n.khalid@deakin.edu.au (Nauman Khalid), Tel: + 61 3 522 78313, Fax: +61 352271040

Abstract

In this study ginseng saponins (GS) were used as natural emulsifiers to formulate and stabilize O/W nanoemulsions loaded with astaxanthin (AST). GS were found to be highly effective at reducing the interfacial tension at the soybean oil-water interfaces, and were capable of producing nano-scaled droplets ($d_{4,3}$ ≈ 125 nm) using a high-pressure homogenizer. The droplet size of the nanoemulsions decreased with increasing emulsifier concentration and homogenization pressure. The nanoemulsions were stable without droplet coalescence against thermal treatment (30-90 ^{o}C, 30 min), and over a narrow range of pH values (7-9). GS-coated droplets were unstable in acidic conditions (pH 3-6) and in the presence of salt (> 25mM NaCl). The formulated nanoemulsions showed slight change in $d_{4,3}$ during 15 days of storage at 5, 25 and 40 ^{o}C. However, the chemical stability strongly depended on the storage temperature, with the lowest level of AST retained in nanoemulsions stored at higher temperature.

Keywords: Astaxanthin; nanoemulsions; ginseng saponins; stability, characterization

1. Introduction

Astaxanthin (AST) is a lipid-soluble carotenoid belonging to the xanthophyll class that is naturally present in some microorganisms and aquatic animals, including algae, trout, krill, crayfish and salmon (Ambati, Phang, Ravi, & Aswathanarayana, 2014). Due to the presence of conjugated double bonds and hydroxyl groups, AST has strong antioxidant activity, which is approximately 10 and 100 times greater than β-carotene and vitamin E, respectively (Miki, 1991; Naguib, 2000). In addition, it has been reported that AST consumption is responsible for numerous biological functions, such as prevention of oxidative stress and macular degeneration, inhibition of some forms of cancers, maintenance of cardiovascular health, enhancement of immune function, and anti-inflammatory activity (Higuera-Ciapara, Felix-Valenzuela, & Goycoolea, 2006). Therefore, there is a considerable interest in fortifying foods and beverages with AST as a nutraceutical ingredient. However, incorporating AST into foods, especially in aqueous-based products, is still facing a number of challenges due to its poor-water solubility, as well as its high susceptibility to chemical degradation when exposed to oxygen, light and heat stress (Liu, McClements, Cao, & Xiao, 2016; Taksima, Limpawattana, & Klaypradit, 2015). Furthermore, similar to other carotenoids, the absorption of AST by the human body is relatively low because of its high hydrophobicity (Kaczor & Baranska, 2016; Yuan, Jin, & Xu, 2012). One attractive and promising way that can overcome these limitations is to encapsulate AST within emulsion-based delivery systems (Liu, McClements, Cao, & Xiao, 2016). Oil-in-water (O/W) conventional emulsions (d>200 nm) and nanoemulsions (d<200 nm) are both thermodynamically unstable systems consisting of two immiscible liquids, in which an oil phase is dispersed as droplets into a water phase (Bai & McClements, 2016). In general, due to their smaller droplet size, nanoemulsions offer higher optical transparency, as well as better physicochemical stability and

bioavailability than conventional emulsions (Kentish, Wooster, Ashokkumar, Balachandran, Mawson, & Simons, 2008).

Selection of an appropriate emulsifier is extremely important for the successful formulation of emulsions in commercial applications. A suitable emulsifier can rapidly adsorb onto the surface of oil droplets and effectively reduce the interfacial tension between oil and water phases, thereby facilitating the disruption of droplets during homogenization (McClements, 2015). In addition, an emulsifier can form an interfacial layer coating on the droplets and generate steric or electrostatic repulsive forces that prevent emulsified droplets from aggregation (McClements, 2015). There are various types of food-grade emulsifiers that are commercially available for producing emulsion-based products in the food industry, including natural emulsifiers (e.g., proteins, phospholipids and polysaccharides) and synthetic emulsifiers (e.g., Tween 80) (McClements, 2015; Shariffa, Tan, Abas, Mirhosseini, Nehdi, & Tan, 2016). Nevertheless, each category of emulsifier differs in its ability to formulate and stabilize emulsions, as well as has its own advantages and disadvantages that make it suitable for particular utilizations. Compared to synthetic emulsifiers, natural emulsifiers attract more attention in the food industry because of increasing demand on consuming “label friendly” products. Earlier researchers have utilized several natural emulsifiers (e.g., sodium caseinate and enzymatically modified lecithin) to stabilize AST-enriched nanoemulsions (Khalid, Shu, Holland, Kobayashi, Nakajima, & Barrow, 2017; Liu, McClements, Cao, & Xiao, 2016). In the current work, we investigated the effectiveness of ginseng saponins as natural emulsifiers for producing and stabilizing O/W nanoemulsions loaded with AST.

Saponins are surface-active components that are composed of one or more hydrophilic sugar moieties covalently bound to a hydrophobic triterpene or steroid

backbone (Oleszek & Hamed, 2010). Previously, researchers have mostly focused on the quillaja saponins (extracted from the *Quillaja saponaria* Molina tree), which are capable of fabricating and stabilizing emulsions containing nano-sized (d < 150 nm) oil droplets (Ozturk, Argin, Ozilgen, & McClements, 2014; Yang, Leser, Sher, & McClements, 2013). Saponins are also found to be rich in ginseng, which is commercially cultivated in China, Japan, Korea and America (Shin, Kwon, & Park, 2015). Ginseng saponins (GS) are well known for their health benefits, such as anti-diabetes, anti-cancer, anti-fatigue, anti-ageing, neuroprotective and hepatoprotective (Francis, Kerem, Makkar, & Becker, 2002; Li & Gong, 2015). Besides their functional effects, GS exhibit surface-active properties due to one or more hydrophilic glycoside moieties (glycone) and a lipophilic triterpene derivative (aglycone) on their molecular structures (Mesgarzadeh, Akbarzadeh, & Rahimi, 2017; Rosa, Silva, Santos, Petenate, & Meireles, 2016). Generally, GS can be classified into neutral or acidic saponins based on the absence or presence of carboxylic acid groups within the sugar moieties (Fuzzati, 2004). Fig. S1 shows representative molecular structures of GS, in which ginsenoside Re and Ro are neutral and acidic saponins, respectively. There have been relatively few studies reporting the utilization of GS as natural emulsifiers to form and stabilize O/W emulsions. Recently, one study showed that annatto seed O/W emulsions could be prepared from GS using an ultrasonic probe (Rosa, Silva, Santos, Petenate, & Meireles, 2016). However, the emulsions obtained in their study had relatively large droplets (d>350 nm) and showed some creaming instability, which might be a limitation in their commercial applications.

In this study, we aimed to characterize the interfacial properties of GS at the oil-water interfaces, and then to investigate the effect of GS concentration and homogenization pressure on the formulation of O/W nanoemulsions loaded with AST. In addition, we

examined the influence of some parameters on the stability of droplets and/or AST in nanoemulsions, including pH, ionic strength, heat treatment and storage temperature.

2. Materials and methods

2.1. Materials

Ginseng saponins extracted from ginseng leaf and stem (GS, saponins 80%) were procured from Hongjiu Biotech Co., Ltd. (Jilin, China). Zanthin® Astaxanthin (purity 10%) was purchased from Valensa International (Eustis, FL, USA). Astaxanthin (purity > 97%) was purchased from Sigma-Aldrich (St. Louis, MO, USA), and was used to prepare the standard curve. Refined soybean oil, sodium hydroxide, hydrochloric acid, sodium azide, sodium chloride, methanol (HPLC grade), and dichloromethane (HPLC grade) were purchased from Wako Pure Chemical Industries, Ltd. (Osaka, Japan). The rest of the chemicals used in the present work were of analytical grade. Milli-Q water was used for preparing all the solutions and emulsions.

2.2. Preparation of AST-loaded nanoemulsions

An oil phase was prepared by dispersing 2% (w/w) Zanthin® Astaxanthin in soybean oil. The mixtures were stirred constantly overnight at ambient room temperature, and then were filtered with a membrane filter (0.45 μm) before formulating the nanoemulsions. An aqueous phase was prepared by dissolving GS (0.08-1.2%, (w/w)) in Milli-Q water. Initially, coarse emulsions containing 5% (w/w) of oil phase and 95% (w/w) of aqueous phase were prepared using a rotor-stator homogenizer (Polytron, PT-3000 Kinematica-AG, Littace, Switzerland) at 8000 rpm for 5 min. Next, fine nanoemulsions were obtained by homogenizing the coarse emulsions through a high-pressure homogenizer (NanoVater, NV200, Yoshida Kikai, Japan) for 4 passes at different pressures (20-100 MPa). In this manuscript, we reported the

concentration of GS in the aqueous phase according to the amount of active emulsifier, rather than the total mass of ingredients present.

2.3. Testing of nanoemulsions stability

The stability of AST-loaded nanoemulsions towards different environmental conditions that can occur in commercial applications was investigated. The samples produced using 0.6% (w/w) GS at fixed homogenization conditions (100 MPa, 4 cycles) were tested.

2.3.1. Effect of thermal treatment

The nanoemulsions were transferred into screw-cap tubes that were then placed in water baths set at different temperatures (30-90 ^{o}C) for 30 min. The resulting samples were then cooled to room temperature prior to analysis.

2.3.2. Effect of pH

The nanoemulsions were adjusted to different pH values (3-9) using 0.1 mol/l HCl or 0.1 mol/l NaOH solutions. The resulting nanoemulsions were then stored at 5 ^{o}C overnight prior to analysis.

2.3.3. Effect of ionic strength

The nanoemulsions were diluted with the same volume of different concentrations of NaCl solution to obtained samples with 2.5% (w/w) of oil and different ionic strength (0-150 mM NaCl). The resulting samples were gently mixed for 30s and then stored at 5 ^{o}C overnight prior to analysis.

2.3.4. Storage stability

The nanoemulsions with 0.02% (w/w) of NaN_3 as preservative were stored at different temperatures of 5, 25, and 40 ^{o}C for a period of 15 days. The droplet size and AST concentration of nanoemulsions were then measured during their storage time.

2.4. Measurement of interfacial tension

The interfacial tension (γ) between soybean oil and water containing GS at different levels (0.0008-0.8%, (w/w)) was measured at ambient temperature using an interfacial tensiometer (PD-W, Kyowa Interfacial Science Co. Ltd., Saitama, Japan), according to the pendant drop method. Briefly, the aqueous solution containing GS was placed in a syringe with a 22G stainless-steel needle, and the soybean oil was placed in a transplant glass cell. A maximum volume of droplet detached from the needle was immersed in the soybean oil, and then the interfacial tension at the soybean oil-water interface was automatically determined by the instrument. Each sample was measured at least 10 times. The surface pressure (π) was calculated using the following equation (1):

$$\pi = \gamma_0 - \gamma \qquad (1)$$

where γ_0 and γ are the interfacial tensions between oil and water measured in the absence and presence of GS, respectively.

2.5. Measurements of droplet size and size distribution

The droplet size and size distribution of nanoemulsions were measured by using a dynamic light scattering particle size analyzer (LS 13320, Beckman Coulter, Brea, USA). This instrument is able to measure droplet size ranging from 0.4 to 2,000 μm. The refractive indices of the aqueous phase and oil phase were set at 1.333 and 1.471, respectively. The mean droplet diameter of nanoemulsions was expressed as Volume mean diameter ($d_{4,3}$) and/or Sauter mean diameter ($d_{3,2}$) in our study. Each sample was measured at least 3 times.

2.6. Measurement of ζ-potential

The electrical charge (ζ-potential) on the emulsified droplets was determined by a Zetasizer (Nano ZS, Malvern Instruments Ltd., Worcestershire, UK) using the Smoluchowski model. The refractive indices of the aqueous phase and oil phase were set at 1.333 and 1.471, respectively. Samples were diluted 100 times with phosphate buffer solutions (5 mM) of appropriate pH and salt concentration prior to analysis. Each sample was measured at least 3 times.

2.7. Quantification of AST concentration in nanoemulsions

The quantification of AST concentration in nanoemulsions followed the procedure as described in our previous study (Khalid, Shu, Holland, Kobayashi, Nakajima, & Barrow, 2017), with minor modification. In brief, 0.2 ml of nanoemulsions were mixed with 9.8 ml of organic solvent (dichloromethane: methanol = 2:1(v/v)) to separate the AST. After extraction, the transparent mixture containing AST was immediately placed in a cuvette, and then the absorbance at 480 nm was measured with a UV/VIS/NIR spectrophotometer (V-570, JASCO Co., Hachioji, Japan). The pure organic solution containing dichloromethane and methanol was used as blank. AST concentration was calculated using a calibration curve (R^2 = 0.9952) created from the aforementioned organic solutions with different amounts of standard AST. Each sample was measured at least 3 times and the results were expressed as AST retention, which is defined by the flowing equation (2):

$$\text{AST retention (\%)} = \frac{C_t}{C_0} \times 100 \qquad (2)$$

where C_0 is the initial AST concentration and C_t is the AST concentration at a specific storage time.

2.8. Statistical analysis

All the experiments were carried out at least two times and the data were reported as means and standard deviations. Statistical analysis was performed by one-way analysis of variance (ANOVA) using Statistix 8.1 software (Tallahassee, USA). Least significant difference (LSD) test with 95% confidence level (p<0.05) was considered statistically significant.

3. Results and discussion

3.1. Interfacial characteristics

It is well known that oil and water are immiscible due to the high interfacial tension between their interfaces. In order to prepare an emulsion successfully, emulsifiers as surface-active agents are needed, due to their ability to adsorb onto the interfaces between oil and water phases and reduce the interfacial tension. In general, the higher and faster decrease in interfacial tension, the greater the ability of an emulsifier to form and stabilize an emulsion (McClements, 2015). We therefore measured the change in interfacial tension as a function of GS concentration, to have a better understanding of its interfacial behaviour at soybean oil-water interfaces (Fig. 1). Initially, the interfacial tension decreased steeply from 21.0 to 8.7 mN/m as the concentration of GS increased from 0.0008% to 0.02% (w/w), which can be attributed to there being more GS molecules available for adsorbing onto the oil-water interfaces and lowering the interfacial tension (Rosen & Kunjappu, 2012). On the other hand, there was a more gradual reduction in interfacial tension at higher GS levels, until a relatively constant value was reached ($\gamma_\infty \approx$ 4.5 mN/m), suggesting that the adsorption of GS molecules onto the oil-water interfaces becomes saturated at high emulsifier levels (Hunter, 2001). The critical micelle concentration (CMC) of an emulsifier was also conveniently determined from the relationship between the interfacial tension and

logarithm of emulsifier concentration using a method reported previously (Bai & McClements, 2016; Varona, Martín, & Cocero, 2009). According to Fig. S2, the estimated CMC value for GS was around 0.049% (w/w) (≈ 0.49 g/l), which is in agreement with those of (0.09 - 0.747 g/l) for saponins extracted from ginseng as reported in previous studies (Mesgarzadeh, Akbarzadeh, & Rahimi, 2017; Ribeiro, Alviano, Barreto, & Coelho, 2013).

We also estimated the surface activity (*K*) of GS by the following relationship (McClements, 2015):

$$K = \frac{1}{C_{1/2}} = \exp\left(-\frac{\Delta G_{ads}}{RT}\right) \quad (3)$$

where, $C_{1/2}$ is GS concentration required to cover half of the available adsorption sites on the interfaces between oil and water, and $\boldsymbol{\Delta G_{ads}}$ is the free energy change related to GS adsorption. To a rough approximation, $C_{1/2}$ can be treated as the GS concentration in which the surface pressure (π) reaches to half of its maximum value (π_∞). In this experiment, we calculated the $C_{1/2}$, *K*, and $\boldsymbol{\Delta G_{ads}}$ based on the surface pressure *versus* GS concentration profile (Fig. S3), and the corresponding data were 0.004% (w/w) (42.2 μM), 23700 M^{-1}, and -10.07 RT, respectively. Here, we used ginsenoside Re (molecular weight = 947 g/mol) as a representative saponin in ginseng to calculate the *K* values. It should be noted that the ginseng extract used in our study may consist of different saponins with different surface activities. Consequently, the values of CMC and *K* reported in our study are only estimates. Overall, the results obtained in this part show that GS can efficiently reduce the interfacial tension between oil-water interfaces even at a relatively low level.

3.2. Effect of GS concentration on AST-loaded nanoemulsion formation

It is important to select an appropriate emulsifier level for producing emulsions with relatively small droplets. We therefore examined the influence of GS concentration on mean droplet diameters ($d_{4,3}$ and $d_{3,2}$) of AST-loaded nanoemulsions produced by a higher-pressure homogenizer at 100 MPa for 4 passes (Fig. 2). The increase in GS levels (from 0.008 to 0.4%, (w/w)) in the aqueous phase led to a rapid reduction in the mean droplet size of emulsified droplets, with $d_{4,3}$ decreasing from 660 to 148 nm, and $d_{3,2}$ decreasing from 400 to 117 nm (Fig. 2a). This result suggests that GS concentration plays an important role in decreasing the droplet size of emulsions. There are two main reasons behind this phenomenon: (i) A relatively higher emulsifier concentration leads to more emulsifier molecules available to locate at the newly created surfaces of oil droplets formed during homogenization; (ii) at relatively higher emulsifier concentration, emulsifier molecules adsorb faster onto the droplet surface, providing improved protection against re-coalescence during homogenization (Ziani, Barish, McClements, & Goddard, 2011). The minimum $d_{4,3}$ (125 nm) and $d_{3,2}$ (105 nm) of nanoemulsions were not significantly (p> 0.05) influenced by the further increase in GS concentration in the aqueous phase (Fig. 2a). This is because the minimum size of oil droplet produced using a high-pressure homogenizer is limited by its disruptive energy, when there are sufficient emulsifier molecules available to cover the newly-created droplet surface (Bai & McClements, 2016; Qian, Decker, Xiao, & McClements, 2011). The measurements of droplet size distribution also indicated that GS-coated droplets became smaller and narrower as GS concentration increased, but they were a constant size at higher concentration of GS (Fig. 2b).

We also calculated the surface load of GS at saturation (Γ) because it is also an important indicator of determining the effectiveness of an emulsifier to form an emulsion. When the droplet size of emulsions was limited by the emulsifier concentration, the minimum amount of emulsifier in the aqueous phase required to

cover all the surfaces of droplets produced is given by equation (4), according to previous studies (Mcclements, 2007; Ozturk, Argin, Ozilgen, & McClements, 2014)

$$C_S = \frac{6 \times \Gamma \times \varphi}{d_{3,2\,min}} \quad (4)$$

where C_S is the concertation of GS in water phase (kg/m^3), Γ is surface load of GS at saturation (kg/m^2), φ is oil volume fraction, and $d_{3,2}$ is the smallest size (m) of emulsified droplet produced. This equation was used to calculate the surface load of GS based on the known oil fraction ($\varphi \approx 0.05$), and measured minimum droplet size ($d_{3,2\,min} \approx 105$ nm) at 0.6% ($C_S \approx 6.0$ kg/m^3) of GS. The calculations suggest that the surface load of GS was approximately 2.1 mg/m^2. It should be noted that this equation is based on the assumption that all the emulsifier molecules in the system can quickly adsorb onto the surface of droplets produced during homogenization. In practice, this assumption maybe not strictly be true, which would lead to some error in the Γ values of GS estimated in our study.

3.3. Effect of homogenization pressure on AST-loaded nanoemulsions formation

It is well known that homogenization conditions (e.g., operating pressure and number of cycles) can impact the size of oil droplets when a high-pressure homogenizer is applied for producing nanoemulsions. We therefore investigated the influence of homogenization pressure (20-120 MPa, 4 cycles) on the characteristics of AST-loaded nanoemulsions stabilized using 0.6% (w/w) GS (Fig. 3). The $d_{4,3}$ of GS-coated droplets decreased from 425 to 127 nm with increasing operating pressure from 20 to 80 MPa (Fig. 3a), due to the magnitude of disruptive energy generated by the instrument as it increases with increasing the homogenization pressure (Schultz, Wagner, Urban, & Ulrich, 2004). On the other hand, the emulsified droplets showed non-significant (p>0.05) reduction in $d_{4,3}$ when the homogenization pressure exceeded

80 MPa. This result was in agreement with previous studies reporting that the mean droplet size remained constant after a certain homogenization pressure (Bai & McClements, 2016; Zhao, Khalid, Shu, Neves, Kobayashi, & Nakajima, 2017). Furthermore, there was a linear decrease in the logarithm of $d_{4,3}$ with the logarithm of the pressure for the production of nanoemulsions using GS (Fig. S4). Previous findings have also indicated that there should be a linear relationship between operating pressure and mean droplet size when the amount of emulsifier is sufficient for stabilizing the nanoemulsions during homogenization (Walstra, 1993). The slope obtained from $\log_{10}(d_{4,3})$ *versus* $\log_{10}(P)$ plots was around -0.71, which is in line with previously reported values (-0.6 to -0.8) for high-pressure homogenizers (Walstra, 2002). It was also found that the width of droplet size distribution became smaller when higher operating pressure was applied for producing the nanoemulsions (Fig. 3b). Overall, the results obtained from this section again suggest that GS are effective at forming nanoemulsions via a high-pressure homogenization method, and the droplet size and size distribution are highly dependent on the operating pressure.

3.4. Effect of heat treatment on AST-loaded nanoemulsions stability

Evaluating the thermal stability is important because emulsion-based products may be exposed to different temperatures during processing, transportation and utilization. The aim of this study was therefore to investigate the influence of heat treatment on the stability of AST-loaded nanoemulsion production using GS (Fig. 4). There was non-significant ($p > 0.05$) change in $d_{4,3}$ and no sign of creaming instability, indicating that the nanoemulsions stabilized by GS were highly stable against thermal processing over the range of temperatures (30-90 ^{o}C) studied (Fig. 4a). Previous studies have reported that the steric repulsion generated by rhamnolipids or sucrose monopalmitate

was not enough to prevent nanoemulsions from aggregration, which is due to that fact the interfacial layer formed by their hydrophilic heads (two sugar groups) is quite thin (Bai & McClements, 2016; Choi, Decker, Henson, Popplewell, Xiao, & McClements, 2011). Similarly, the steric repulsion generated by GS, which contains small sugar groups, would be expected to be weak and insufficient to resist the attractive forces (e.g., van der Waals and hydrophobic), that could lead to instability of nanoemulsions. A number of previous publications have reported that saponin-based emulsifiers stabilize emulsions mainly by electrostatic repulsion mechanisms, which is due to the presence of carboxylic acid groups in their chemical structure (Ralla, Salminen, Edelmann, Dawid, Hofmann, & Weiss, 2017; Yang, Leser, Sher, & McClements, 2013). We therefore hypothesized that electrostatic repulsion plays an important role for the stability of GS-coated droplets, since some types of saponins in ginseng also have carboxyl groups on their molecules as described earlier. Indeed, the ζ-potential measurements confirmed that all of the nanoemulsions had a similar and strongly negative charge of around -35 mV after thermal treatment (Fig. 4b). Thus, the observation of excellent thermal stability for GS-coated droplets could be attributed to the strong electrostatic repulsion between them.

3.5. Effect of pH on AST-loaded nanoemulsions stability

Investigating the pH stability of emulsified droplets is important because commercial foods and beverages often exhibit different pH values. Thus, the purpose of this experiment was to examine the influence of pH on the stability of AST-loaded nanoemulsions stabilized using GS (Fig. 5). The nanoemulsions were highly stable without evidence of change in $d_{4,3}$ and phase separation at relatively high pH values of 7 to 9 (Fig. 5a). However, the nanoemulsions stabilized by GS started to become

unstable with a significant ($p < 0.05$) increase in $d_{4,3}$ at pH 4-6 and became highly unstable with strong oiling-off at pH 3, suggesting that droplet coalescence had occurred under acidic conditions. In order to provide some potential mechanisms for the pH-instability of GS-coated droplets, the pH dependence of ζ-potential of the nanoemulsions was therefore examined (Fig. 5b). The electrical charge of GS-stabilized droplets depended greatly on the pH, with the magnitude of ζ-potential going from strongly negative (≈ -40 mV) at pH 9 to slightly negative (≈ -13 mV) at pH 4 (Fig. 5b). The poor stability of nanoemulsions at low pH can be because repulsion generated by GS is insufficient for preventing the droplets from coming together, thereby leading to droplet coalescence. As mentioned earlier, GS stabilizes the nanoemulsions by electrostatic repulsion, which might be due to the presence of carboxylic acid groups in the molecular structure of GS. It has been reported that the carboxylic acid groups in saponin-based emulsifiers typically have a p*K*a value of around 3.5 (Ralla, Salminen, Edelmann, Dawid, Hofmann, & Weiss, 2017; Yang, Leser, Sher, & McClements, 2013), which could account for the large decrease in electrical charge observed around this pH value. The carboxylic acid group tends to be strongly charged at high pH values (pH ≫ pKa), due to the dissociation effect (COO^-), and uncharged at low pH values (pH << p*K*a), due to the protonation effect (COOH).

3.6. Effect of ionic strength on AST-loaded nanoemulsion stability

Testing the stability of nanoemulsions against ionic strength is also important as different commercial beverages contain different levels of minerals. The aim of this section was therefore to study the influence of NaCl concentration on the stability of AST-loaded nanoemulsions stabilized using GS (Fig. S5). Good stability of nanoemulsions was only observed at low levels of NaCl (≤ 25 mM), since there was

no change in $d_{4,3}$ of GS-coated droplets and visible appearance (Fig. S5a). However, the nanoemulsions were very sensitive and prone to droplet coalescence at higher salt concentration, and they became highly unstable with a large amount of oil phase separation being observed at ≥ 125 mM NaCl. Apparently, the addition of salt led to the GS-formed interfacial layer being more flexible and prone to disruption. This effect can be attributed to the presence of Na^+ cations decreasing the electrostatic repulsion between the negatively charged droplets, thereby leading to droplet coalescence and instability (McClements, 2015). This explanation was confirmed by ζ-potential measurements, which showed the electrical charge on the GS-coated droplets decreased with increasing NaCl concentration (Fig. S5b).

3.7. Storage stability

Finally, we investigated the storage stability of nanoemulsions by placing them at different temperatures (5, 25, and 40 ^{o}C). The stability was evaluated based on the change in $d_{4,3}$ and AST retention in 0.6% (w/w) GS-stabilized nanoemulsions during 15 days of storage (Fig. 6).

3.7.1. Physical stability

As shown in Fig. 6a, there was slight change in the $d_{4,3}$ of AST-loaded nanoemulsions during 15 days of storage, regardless of the storage temperature studied. In addition, there were slight changes of creaming instability in all the samples (data not shown). These results indicated that the AST-loaded nanoemulsions produced by GS were physically stable at these storage temperatures (5, 25 and 45 ^{o}C) for at least 15 days. There are three main reasons accounting for the good storage stability of GS-coated droplets in nanoemulsions: (i) The droplets produced from GS were nano-scaled, which can prevent creaming instability (Tadros, Izquierdo, Esquena, & Solans, 2004);

(ii) the nanoemulsions obtained from water-insoluble oil (soybean oil used in our study) are relatively stable against the destabilizing effects of Ostwald ripening (Shu, Khalid, Zhao, Neves, Kobayashi, & Nakajima, 2016); (iii) the electrostatic repulsion generated by GS presumably is strong enough to prevent nanoemulsion instability.

3.7.2. AST stability

The primary nanoemulsions stabilized by GS contained 90 ± 2.5 μg/ml AST (data not shown), which was regarded as 100% AST retention at day 0. The concentration of AST in freshly prepared GS-stabilized nanoemulsions was slightly lower than the theoretical concentration (≈ 100μg/ml), which could be attributed to some AST being oxidized by free radicals formed during high-pressure homogenization (Liu, McClements, Cao, & Xiao, 2016). There were clear differences in AST stability between nanoemulsions stored at different temperatures (Fig. 6b). The nanoemulsions incubated at 5 ^{o}C were the most chemically stable, with only a slight AST loss of 2.5% after 15 days of storage. In contrast, the nanoemulsions stored at 40 ^{o}C showed significant AST loss of 64%. Elevated temperatures increase the kinetic energy of the nanoemulsion system, thereby accelerating the collisions of AST-loaded droplets with pro-oxidants, as well as the rate of oxidation reactions (Tamjidi, Shahedi, Varshosaz, & Nasirpour, 2014).

4. Conclusions

In this study, we performed a detailed investigation of the interfacial properties of the natural emulsifiers ginseng saponins, and their ability to formulate and stabilize a nanoemulsion-based delivery system for encapsulating astaxanthin. The results demonstrated that GS were highly surface active and could successfully formulate AST-loaded nanoemulsions via a high-pressure homogenization method. The stability

of GS-coated droplets was not strongly affected by thermal treatment (30-90 ^{o}C, 30 min). Conversely, pH and ionic strength had marked impacts on the physical stability of nanoemulsions, with droplet coalescence occurring under acidic conditions (pH 3-6) or at high salt level (> 25mM, NaCl). These effects were attributed to low pH or the presence of salt (presumably Na^{+} ions) leading to a reduction in the magnitude of the electrostatic repulsion between GS-coated droplets. These instabilities may limit the application of GS as natural emulsifiers in some emulsion-based products. Thus, further studies are required to improve the pH and salt stability of nanoemulsions by using other methods, such as multiple nanoemulsions and combined emulsifiers. The nanoemulsions had a good long-term stability against droplet growth and creaming during 15 days of storage at various temperatures (5, 25, and 40 ^{o}C). However, the rate of AST degradation in nanoemulsions stored at higher temperature was much faster than those stored at lower temperature, which is probably a result of thermal instability of AST. We believe these results are important for designing a nanoemulsion-based system for delivering oil-soluble bioactive compounds using label-friendly materials. Further studies are required to systematically analyze the chemical structures of this commercial complex saponins extract to gain a better understanding of how specific components influence emulsifying activity and the stability of nanoemulsions.

Figure captions

Fig. 1. Influence of GS concentration on the interfacial tension measured at soybean oil-water interfaces. Different letters indicate significant difference at a 95% probability level. *Note*: the emulsifier concentration for GS is the active component.

Fig. 2. Influence of GS concentration on droplet characteristics of AST-loaded nanoemulsions produced using fixed homogenization conditions (100 Mpa, 4 passes). (a) mean droplet diameter ($d_{4,3}$ and $d_{3,2}$) and (b) droplet size distributions of nanoemulsions. Different lowercase letters indicate significant difference at a 95% probability level between the $d_{4,3}$ of nanoemulsions. Different uppercase letters indicate significant difference at a 95% probability level between the $d_{3,2}$ of nanoemulsions.

Fig. 3. Influence of homogenization pressure (4 passes) on droplet characteristics of AST-loaded nanoemulsions stabilized using 0.6% (w/w) GS. (a) mean droplet diameter ($d_{4,3}$) and (b) droplet size distributions of nanoemulsions. Different letters indicate significant difference at a 95% probability level.

Fig. 4. Influence of thermal treatment on the physical stability of AST-loaded nanoemulsions (GS, 0.6% (w/w)) produced using fixed homogenization conditions (100 Mpa, 4 passes). (a) mean droplet diameter ($d_{4,3}$) and (b) ζ-potential of nanoemulsions. Different letters indicate significant difference at a 95% probability level.

Fig. 5. Influence of pH on the physical stability of AST-loaded nanoemulsions (GS, 0.6% (w/w)) produced using fixed homogenization conditions (100 MPa, 4 passes). (a) mean droplet diameter ($d_{4,3}$) and (b) ζ-potential of nanoemulsions. Different letters indicate significant difference at a 95% probability level.

Fig. 6. Influence of storage temperature on the stability of AST-loaded nanoemulsions (GS, 0.6% (w/w)) produced using fixed homogenization conditions (100 MPa, 4 passes). (a) physical stability and (b) AST stability of nanoemulsions.

References

Ambati, R. R., Phang, S.-M., Ravi, S., & Aswathanarayana, R. G. (2014). Astaxanthin: sources, extraction, stability, biological activities and its commercial applications—a review. *Marine drugs, 12*(1), 128-152.

Bai, L., & McClements, D. J. (2016). Formation and stabilization of nanoemulsions using biosurfactants: Rhamnolipids. *Journal of colloid and interface science, 479*, 71-79.

Choi, S. J., Decker, E. A., Henson, L., Popplewell, L. M., Xiao, H., & McClements, D. J. (2011). Formulation and properties of model beverage emulsions stabilized by sucrose monopalmitate: Influence of pH and lyso-lecithin addition. Food research international, 44(9), 3006-3012.

Francis, G., Kerem, Z., Makkar, H. P., & Becker, K. (2002). The biological action of saponins in animal systems: a review. *British journal of nutrition, 88*(6), 587-605.

Fuzzati, N. (2004). Analysis methods of ginsenosides. Journal of Chromatography B, 812(1), 119-133

Higuera-Ciapara, I., Felix-Valenzuela, L., & Goycoolea, F. M. (2006). Astaxanthin: A review of its chemistry and applications. *Critical Reviews in Food Science and Nutrition, 46*(2), 185-196.

Hunter, R. J. (2001). *Foundations of colloid science*: Oxford University Press.

Kaczor, A., & Baranska, M. (2016). *Carotenoids: Nutrition, Analysis and Technology*: John Wiley & Sons.

Kentish, S., Wooster, T., Ashokkumar, M., Balachandran, S., Mawson, R., & Simons, L. (2008). The use of ultrasonics for nanoemulsion preparation. *Innovative Food Science & Emerging Technologies, 9*(2), 170-175.

Khalid, N., Shu, G., Holland, B. J., Kobayashi, I., Nakajima, M., & Barrow, C. J. (2017). Formulation and characterization of O/W nanoemulsions encapsulating high concentration of astaxanthin. *Food Research International*. In press.

Li, K.-K., & Gong, X.-J. (2015). A review on the medicinal potential of Panax ginseng saponins in diabetes mellitus. *Rsc Advances, 5*(59), 47353-47366.

Liu, X. J., McClements, D. J., Cao, Y., & Xiao, H. (2016). Chemical and Physical Stability of Astaxanthin-Enriched Emulsion-Based Delivery Systems. *Food Biophysics, 11*(3), 302-310.

Mcclements, D. J. (2007). Critical review of techniques and methodologies for characterization of emulsion stability. *Critical Reviews in Food Science and Nutrition, 47*(7), 611-649.

McClements, D. J. (2015). *Food emulsions: principles, practices, and techniques*: CRC press.

Mesgarzadeh, I., Akbarzadeh, A. R., & Rahimi, R. (2017). Surface-Active Properties of Solvent-Extracted Panax ginseng Saponin-Based Surfactants. *Journal of Surfactants and Detergents, 20*(3), 609-614.

Miki, W. (1991). Biological functions and activities of animal carotenoids. *Pure and Applied Chemistry, 63*(1), 141-146.

Naguib, Y. M. (2000). Antioxidant activities of astaxanthin and related carotenoids. *Journal of Agricultural and Food Chemistry, 48*(4), 1150-1154.

Oleszek, W., & Hamed, A. (2010). Saponin-based surfactants. *Surfactants from Renewable Resources*, John Wiley & Sons Ltd., United Kingdom, 239-248.

Ozturk, B., Argin, S., Ozilgen, M., & McClements, D. J. (2014). Formation and stabilization of nanoemulsion-based vitamin E delivery systems using natural surfactants: Quillaja saponin and lecithin. *Journal of Food Engineering, 142*, 57-63.

Qian, C., Decker, E. A., Xiao, H., & McClements, D. J. (2011). Comparison of biopolymer emulsifier performance in formation and stabilization of orange oil-in-water emulsions. *Journal of the American Oil Chemists' Society, 88*(1), 47-55.

Ralla, T., Salminen, H., Edelmann, M., Dawid, C., Hofmann, T., & Weiss, J. (2017). Sugar Beet Extract (Beta vulgaris L.) as a New Natural Emulsifier: Emulsion Formation. *Journal of Agricultural and Food Chemistry, 65*(20), 4153-4160.

Ribeiro, B. D., Alviano, D. S., Barreto, D. W., & Coelho, M. A. Z. (2013). Functional properties of saponins from sisal (Agave sisalana) and juá (Ziziphus joazeiro): critical micellar concentration, antioxidant and antimicrobial activities. *Colloids and Surfaces A: Physicochemical and Engineering Aspects, 436*, 736-743.

Rosa, M. T. M., Silva, E. K., Santos, D. T., Petenate, A. J., & Meireles, M. A. A. (2016). Obtaining annatto seed oil miniemulsions by ultrasonication using aqueous extract from Brazilian ginseng roots as a biosurfactant. *Journal of Food Engineering, 168*, 68-78.

Rosen, M. J., & Kunjappu, J. T. (2012). *Surfactants and interfacial phenomena*: John Wiley & Sons.

Schultz, S., Wagner, G., Urban, K., & Ulrich, J. (2004). High‐pressure homogenization as a process for emulsion formation. *Chemical Engineering & Technology, 27*(4), 361-368.

Shariffa, Y. N., Tan, T. B., Abas, F., Mirhosseini, H., Nehdi, I. A., & Tan, C. P. (2016). Producing a lycopene nanodispersion: The effects of emulsifiers. *Food and Bioproducts Processing, 98*, 210-216.

Shin, B.-K., Kwon, S. W., & Park, J. H. (2015). Chemical diversity of ginseng saponins from Panax ginseng. *Journal of ginseng research, 39*(4), 287-298.

Shu, G., Khalid, N., Zhao, Y., Neves, M. A., Kobayashi, I., & Nakajima, M. (2016). Formulation and stability assessment of ergocalciferol loaded oil-in-water nanoemulsions: Insights of emulsifiers effect on stabilization mechanism. *Food Research International, 90*, 320-327.

Tadros, T., Izquierdo, P., Esquena, J., & Solans, C. (2004). Formation and stability of nano-emulsions. *Advances in colloid and interface science, 108*, 303-318.

Taksima, T., Limpawattana, M., & Klaypradit, W. (2015). Astaxanthin encapsulated in beads using ultrasonic atomizer and application in yogurt as evaluated by consumer sensory profile. *LWT-Food Science and Technology, 62*(1), 431-437.

Tamjidi, F., Shahedi, M., Varshosaz, J., & Nasirpour, A. (2014). EDTA and α‐tocopherol improve the chemical stability of astaxanthin loaded into nanostructured lipid carriers. *European Journal of Lipid Science and Technology, 116*(8), 968-977.

Varona, S., Martín, Á., & Cocero, M. J. (2009). Formulation of a natural biocide based on lavandin essential oil by emulsification using modified starches. *Chemical Engineering and Processing: Process Intensification, 48*(6), 1121-1128.

Walstra, P. (1993). Principles of emulsion formation. *Chemical Engineering Science, 48*(2), 333-349.

Walstra, P. (2002). *Physical chemistry of foods*: CRC Press.

Yang, Y., Leser, M. E., Sher, A. A., & McClements, D. J. (2013). Formation and stability of emulsions using a natural small molecule surfactant: Quillaja saponin (Q-Naturale®). *Food Hydrocolloids, 30*(2), 589-596.

Yuan, C., Jin, Z., & Xu, X. (2012). Inclusion complex of astaxanthin with hydroxypropyl-β-cyclodextrin: UV, FTIR, 1 H NMR and molecular modeling studies. *Carbohydrate polymers, 89*(2), 492-496.

Zhao, Y., Khalid, N., Shu, G., Neves, M. A., Kobayashi, I., & Nakajima, M. (2017). Formulation and characterization of O/W emulsions stabilized using octenyl succinic anhydride modified kudzu starch. *Carbohydrate polymers*, *176*, 91-98.

Ziani, K., Barish, J. A., McClements, D. J., & Goddard, J. M. (2011). Manipulating interactions between functional colloidal particles and polyethylene surfaces using interfacial engineering. *Journal of colloid and interface science, 360*(1), 31-38.

Fig. 1

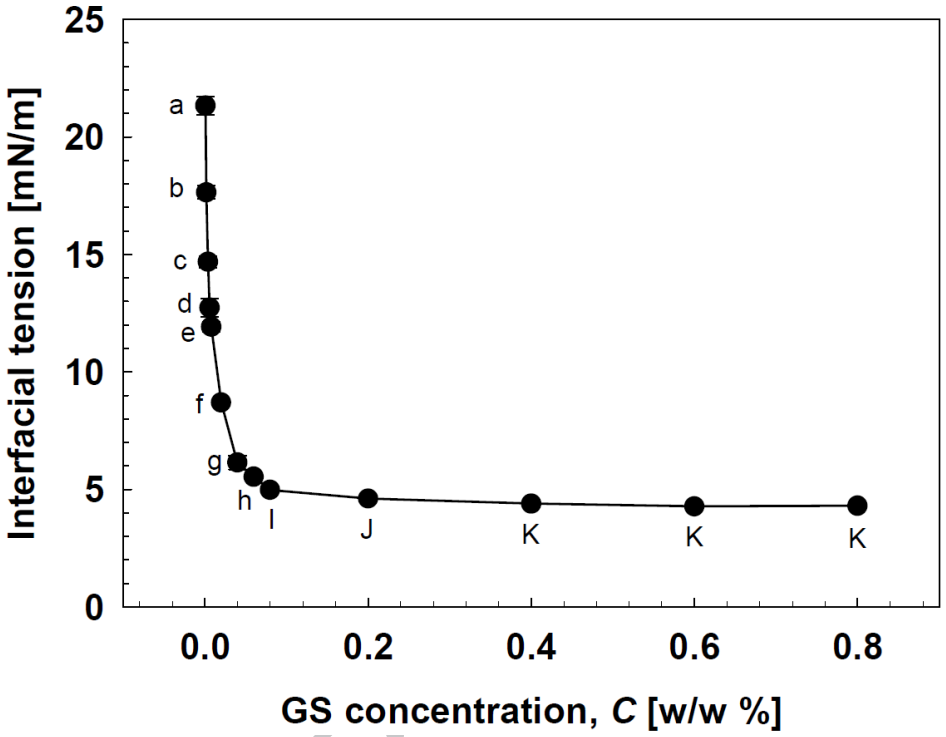

Fig. 2

(a)

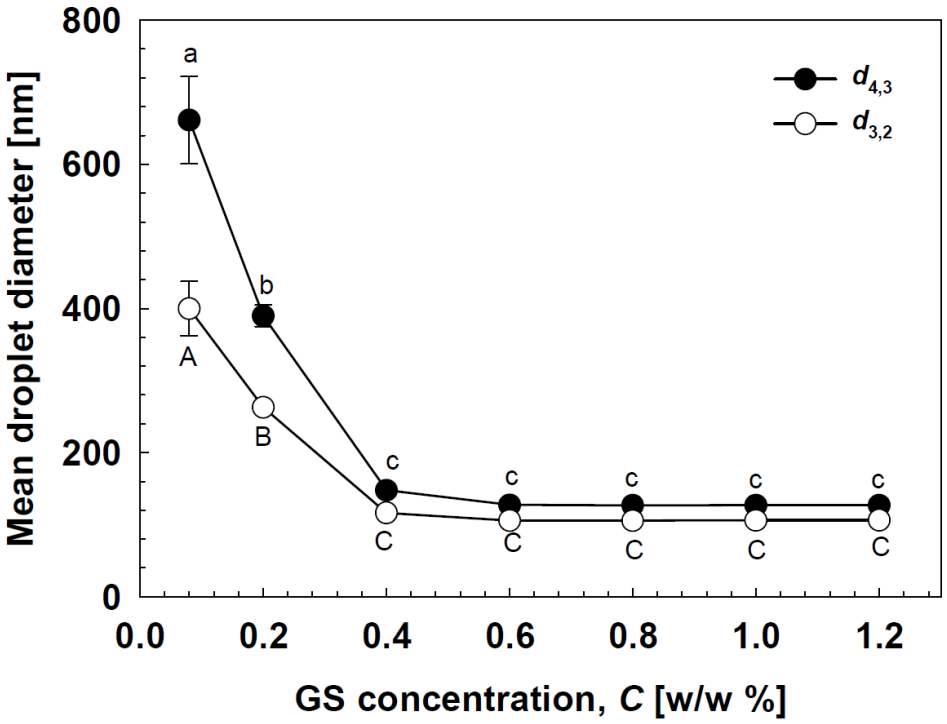

(b)

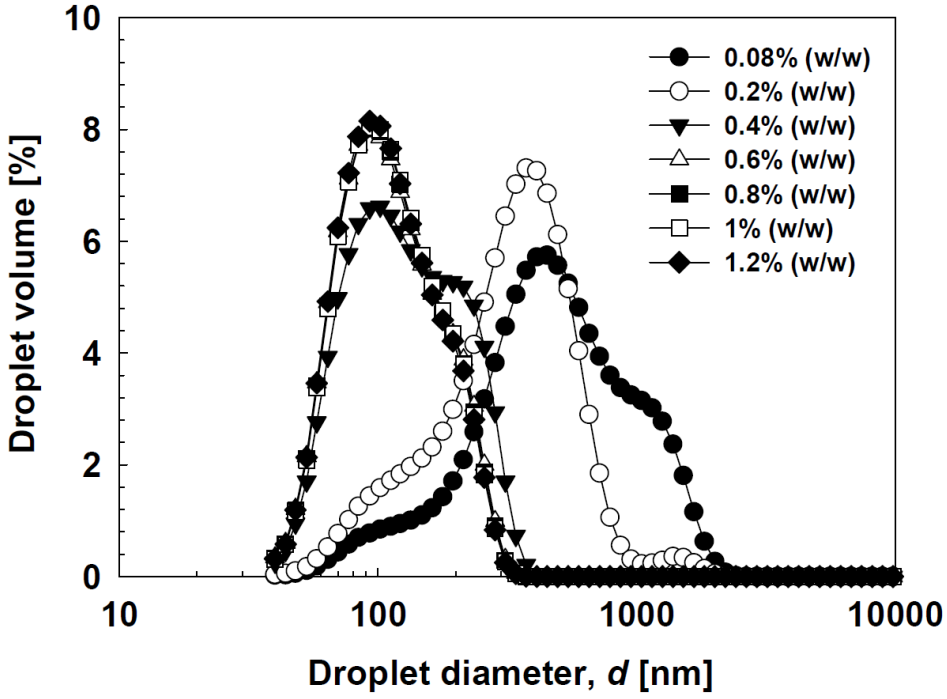

Fig. 3

(a)

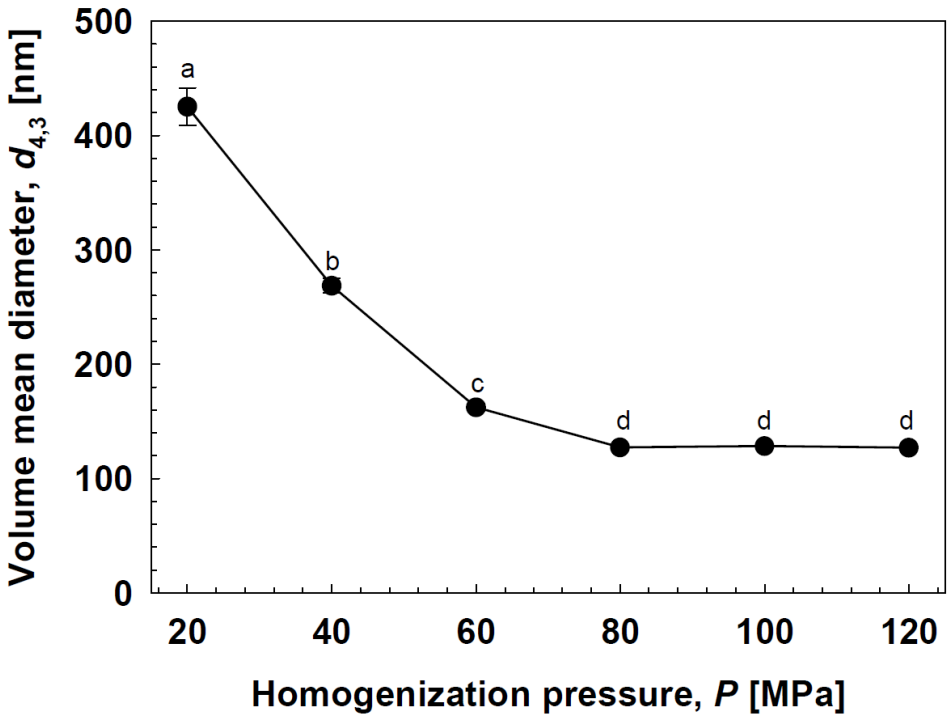

(b)

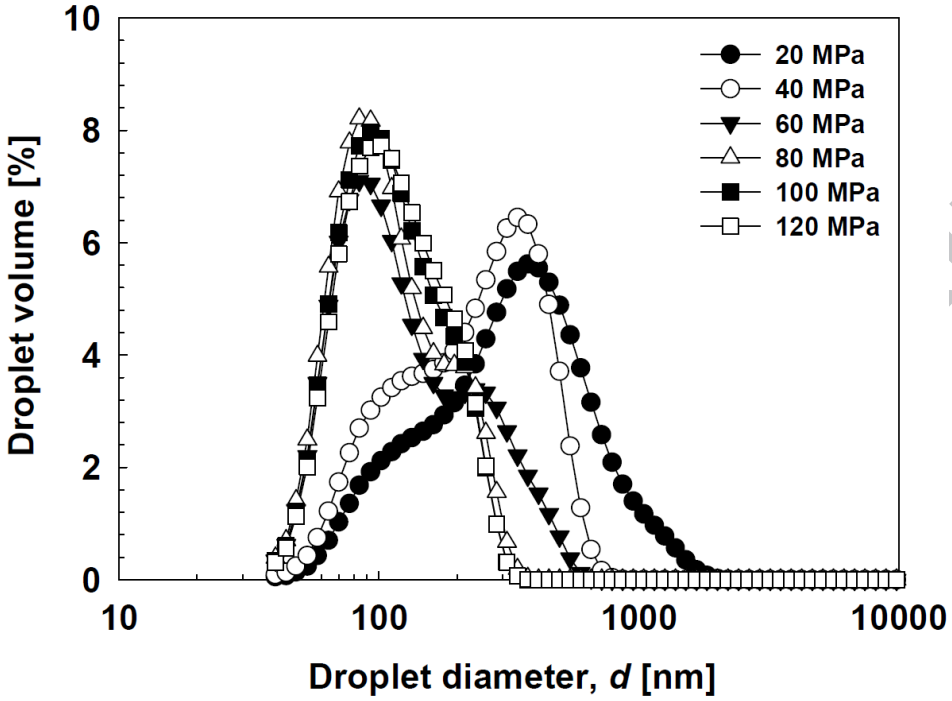

Fig. 4

(a)

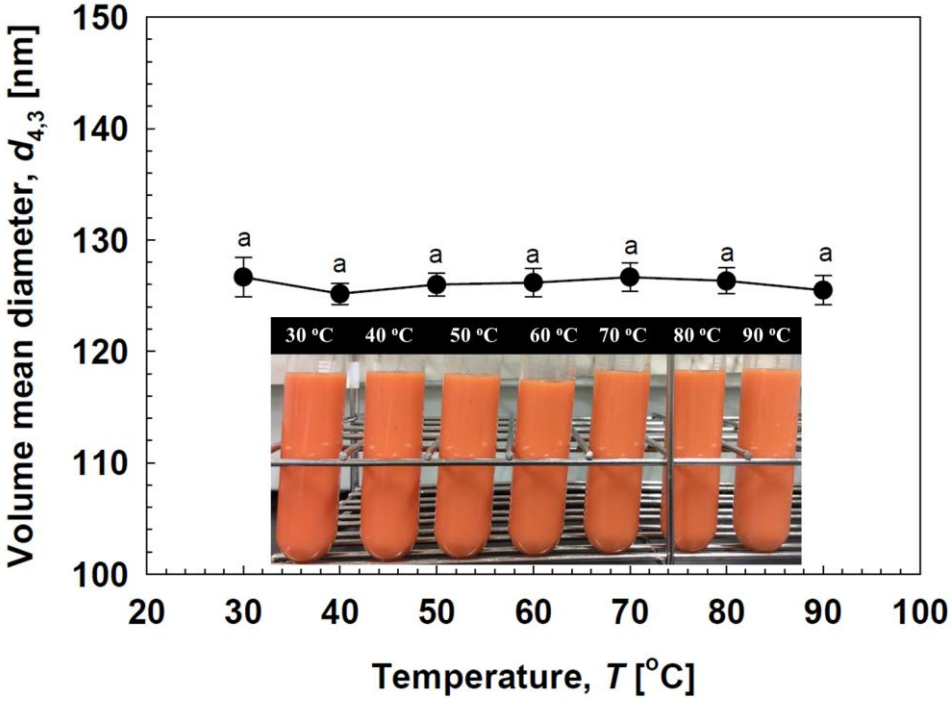

(b)

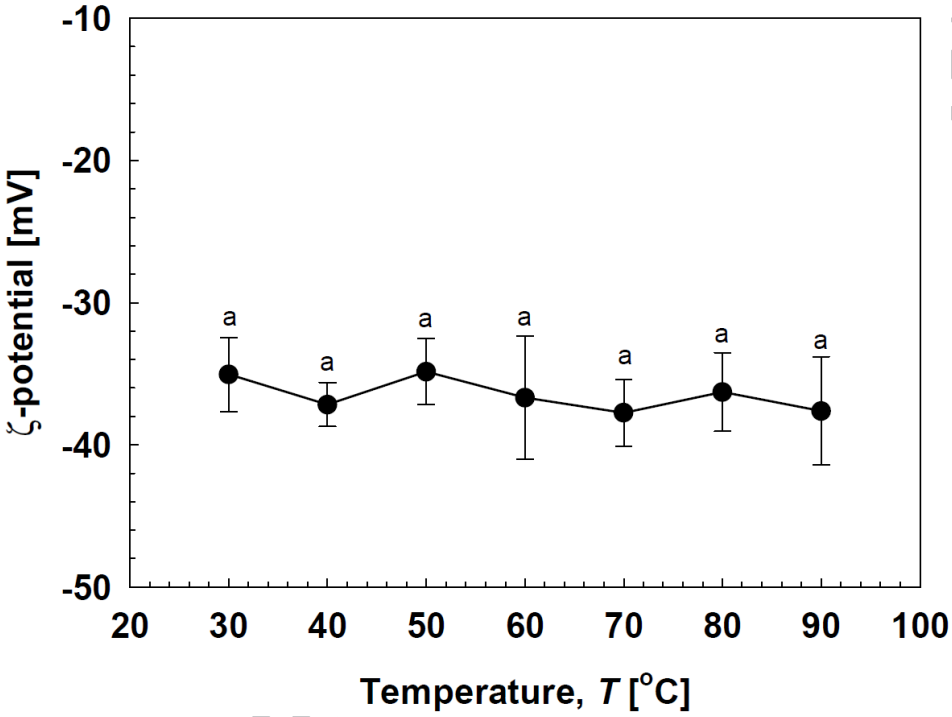

Fig. 5

(a)

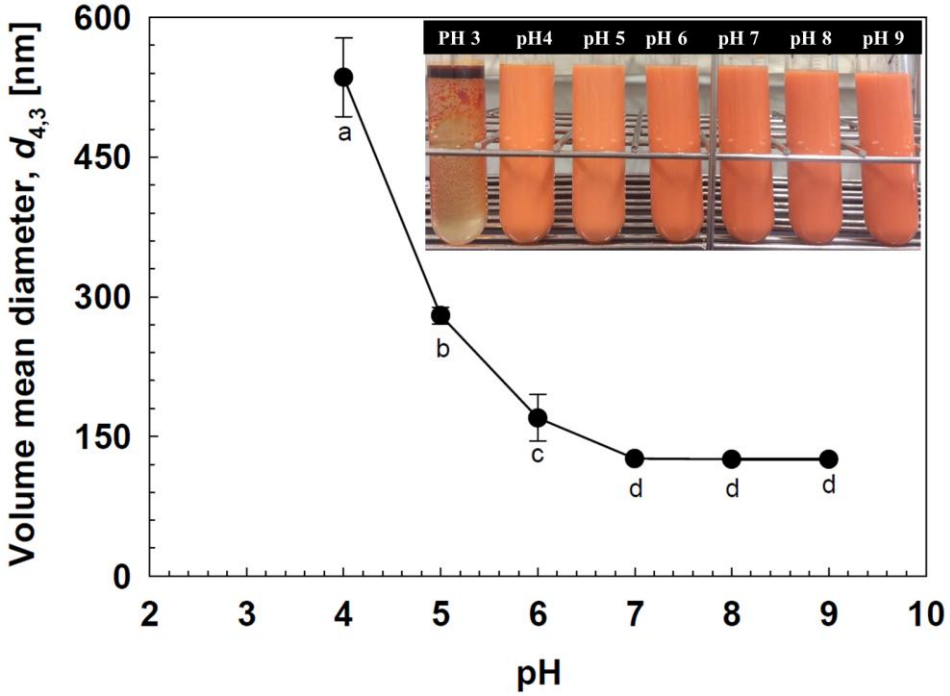

(b)

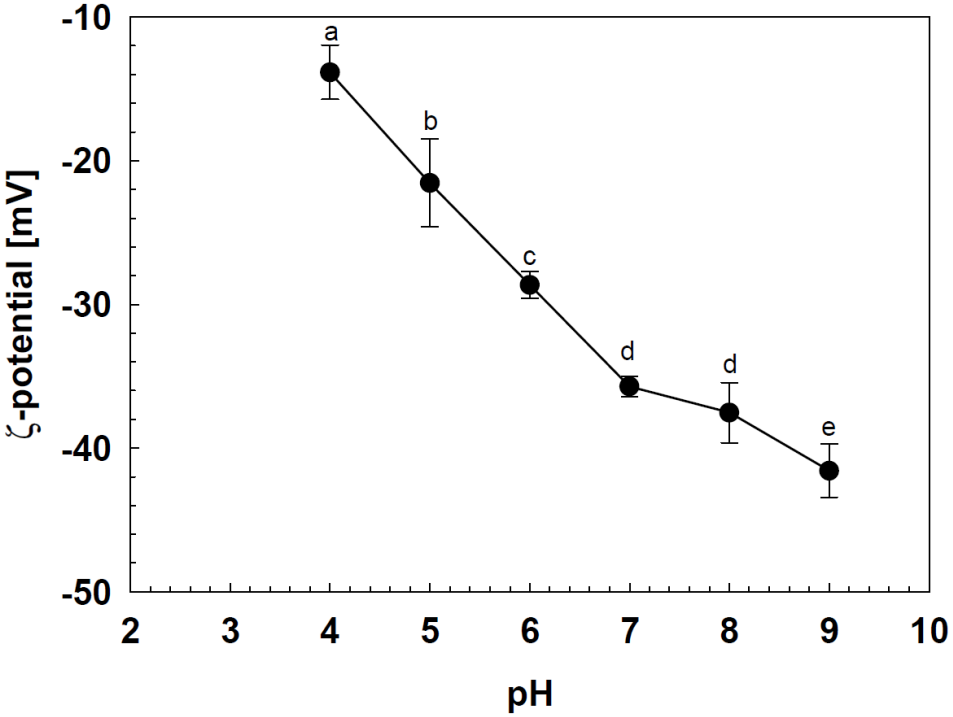

Fig. 6

(a)

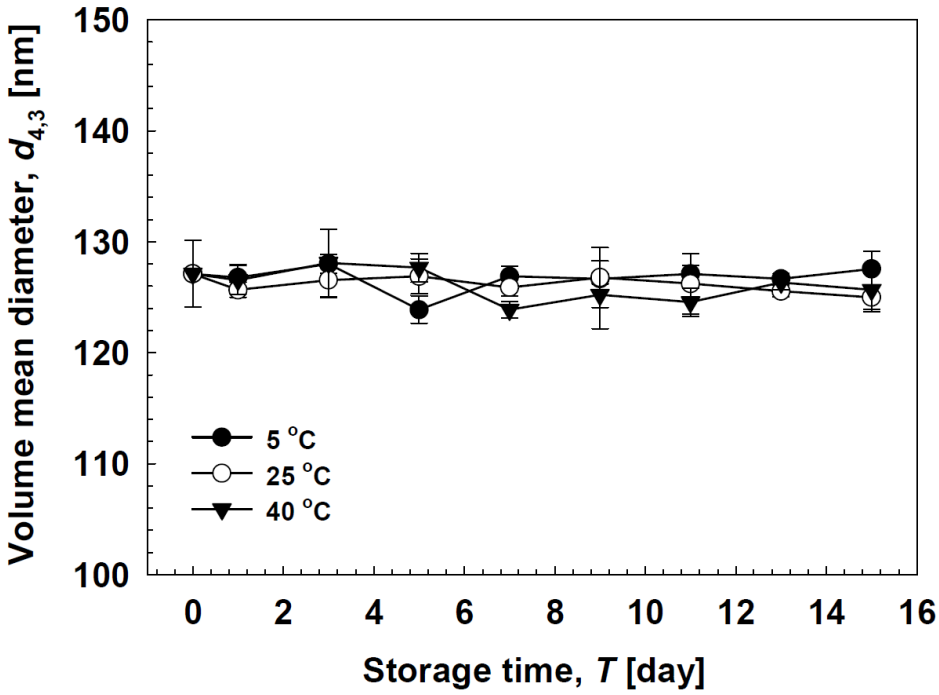

(b)

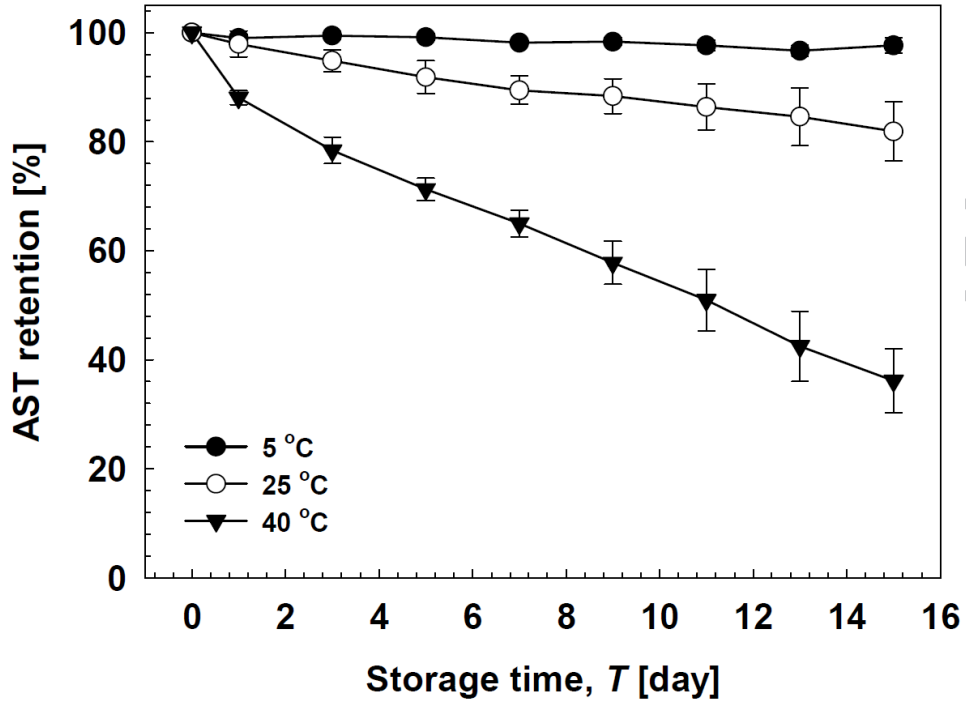

Highlights

- Ginseng saponins (GS) are natural emulsifiers that exhibit strong surface activity
- Astaxanthin-loaded nanoemulsions were successfully formulated using GS
- GS-coated droplets were stable against heat treatment (30-90 ^{o}C, 30 min)
- GS-coated droplets were unstable at pH 3-6, and with salt addition (> 25mM NaCl)
- Nanoemulsions stored at low temperature (5 ^{o}C) had excellent astaxanthin stability